4.7 Testing of a two-ray channel model

In this research, the performance of the two-ray Rayleigh channel model for both urban and suburban areas is evaluated using the following parameters listed in Table 4.2. Also the magnitude and phase response of a simulated two-ray Rayleigh channel for vehicle speed in ranging from 10 km/hr to 80 km/hr are illustrated in Figures 4.4-4.7

Table 4.2 Simulated channel parameters

Urban	Suburban
Carrier Freq: 915 MHz	Carrier Freq: 915 MHz
C/D: 5 dB	C/D: 5 dB
τ: 5 ~ 7 μs	τ: 7 ~ 11 μs
Vehicle Speed: 10 ~ 80 km/hr	Vehicle Speed: 10 ~ 80 km/hr
Doppler Shift: 9 ~ 68 Hz	Doppler Shift: 9 ~ 68 Hz

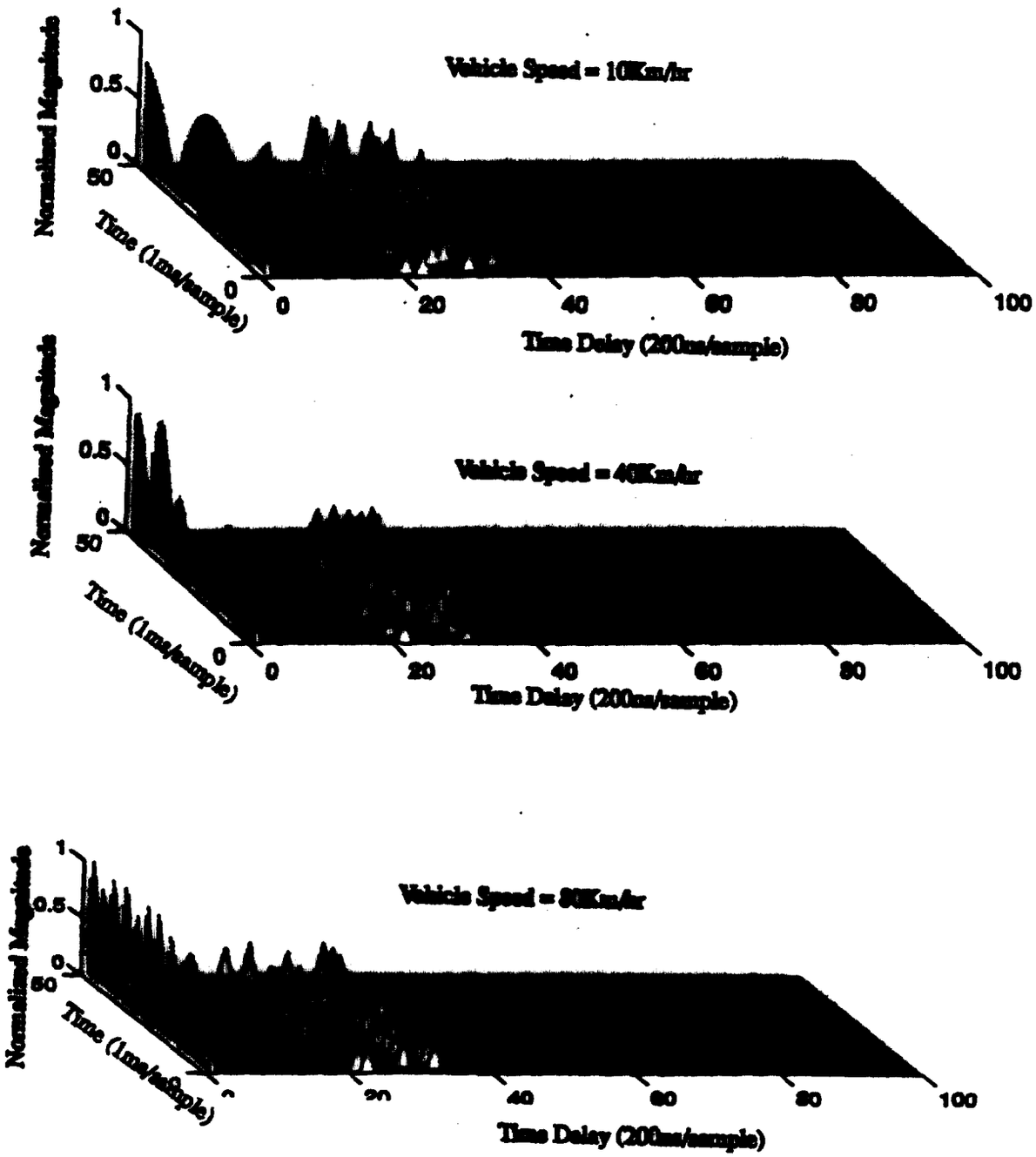

Figure 4.4 The normalized magnitudes of channel impulse responses for an urban area.

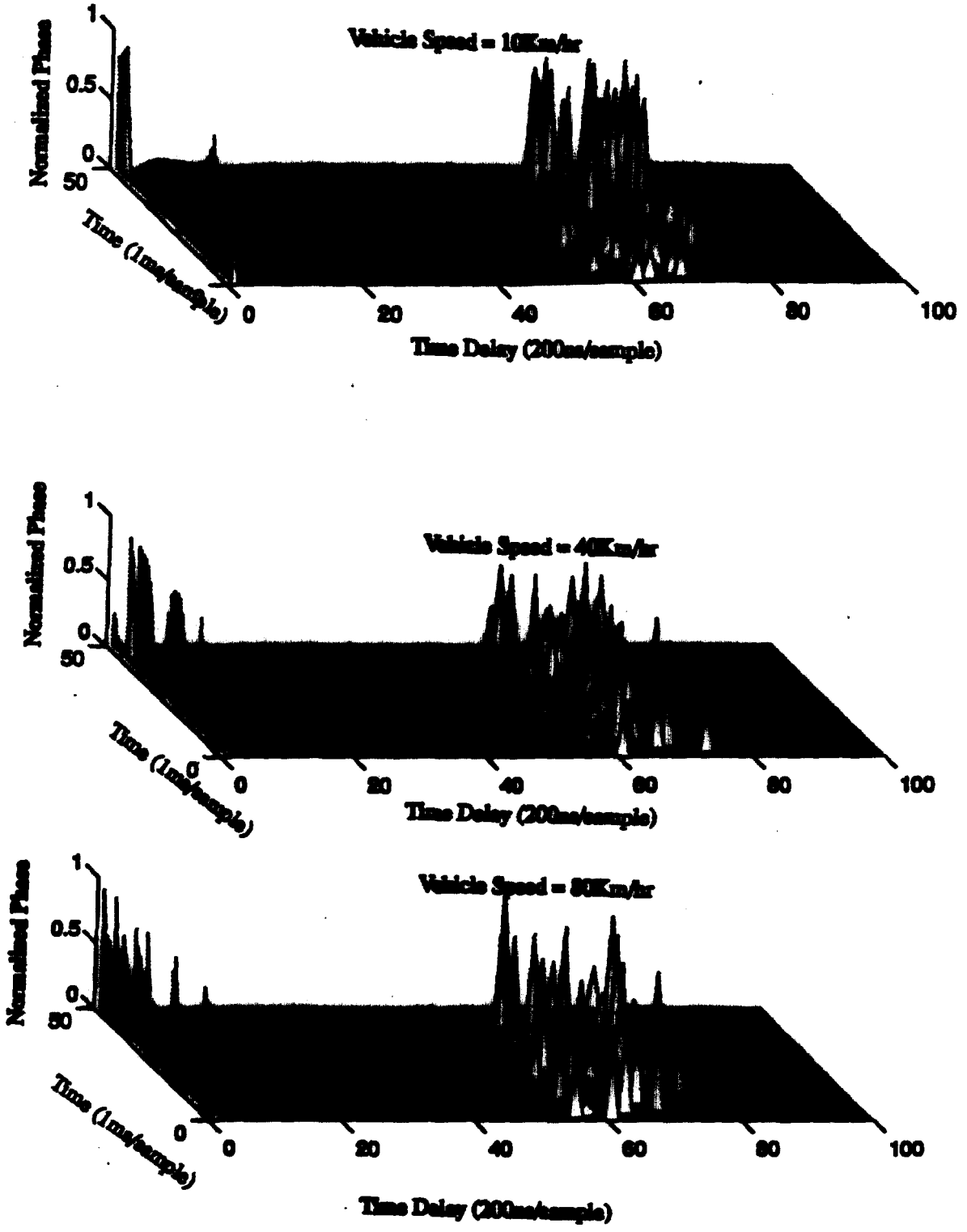

Figure 4.5 The normalized phases of channel impulse responses for an urban area.

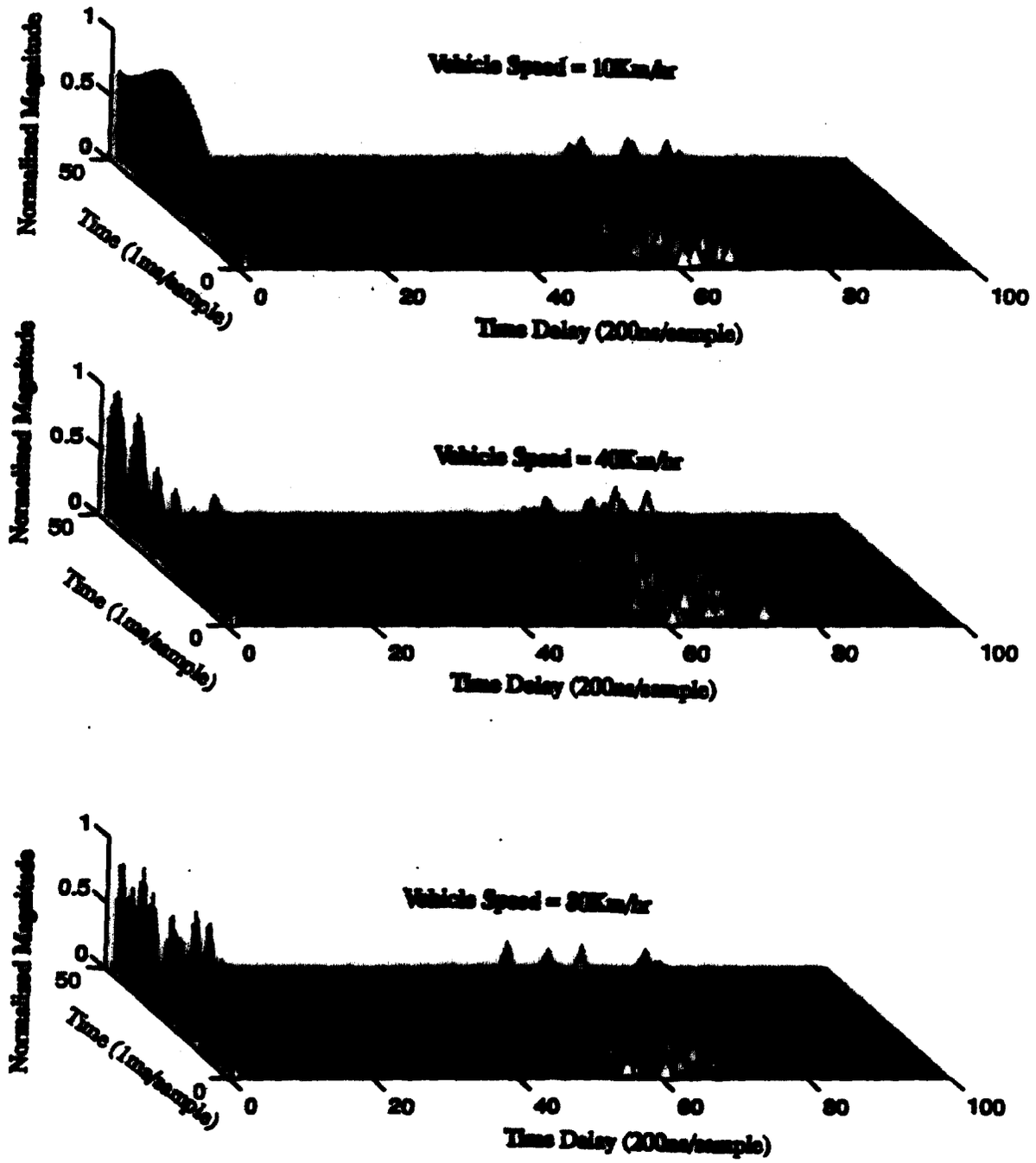

Figure 4.6 The normalized magnitudes of channel impulse responses for a suburban area.

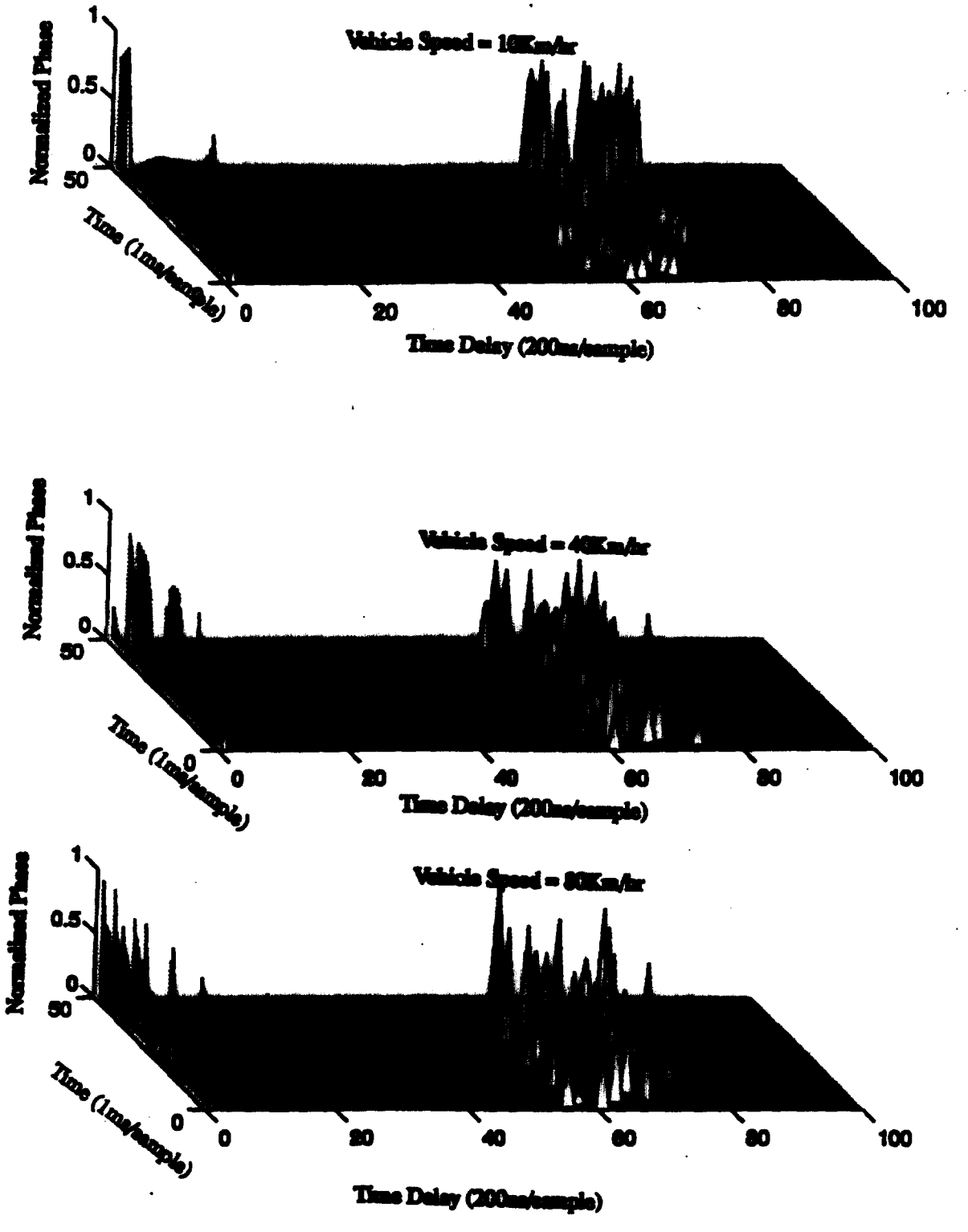

Figure 4.7 The normalized phases of channel impulse responses for a suburban area.

4.8 Simulated system model

In this research, we employed a DS/SS software simulator developed by the Mobile and Portable Radio Research Group (MPRG) to evaluate the effects of RF propagation on the performance of DS/SS AVM systems for different mobile environments. In order to illustrate the effects of multipath propagation with realistic channel coding and interleaving we have modeled the candidate system after the well-studied IS-95 standard for cellular telephone. Because this system has a relatively narrow 1.25 MHz bandwidth, it serves to illustrate the effects of multipath on spread-spectrum systems with relatively narrow bandwidth.

A block diagram of the system model used in the simulation is shown in Figure 4.8 . The system parameters of transceiver used in the simulated models are also listed in Table 4.3.

Table 4.3 Simulated parameters of transceiver

Modulation Type	QPSK
Source Data	Random
Data Rate	1200 ~ 9600 bps
Chip Rate	1.2288 Mcps
FEC coding	Convolutional, r=1/2, K=9
Block Interleaving	24 x 16 array
Processing Gain	128 or 21 dB
Pulse Shaping	Raise Cosine Filter (FIR)
RAKE Receiver	3
Number of Users	20
Eb/No	10 dB

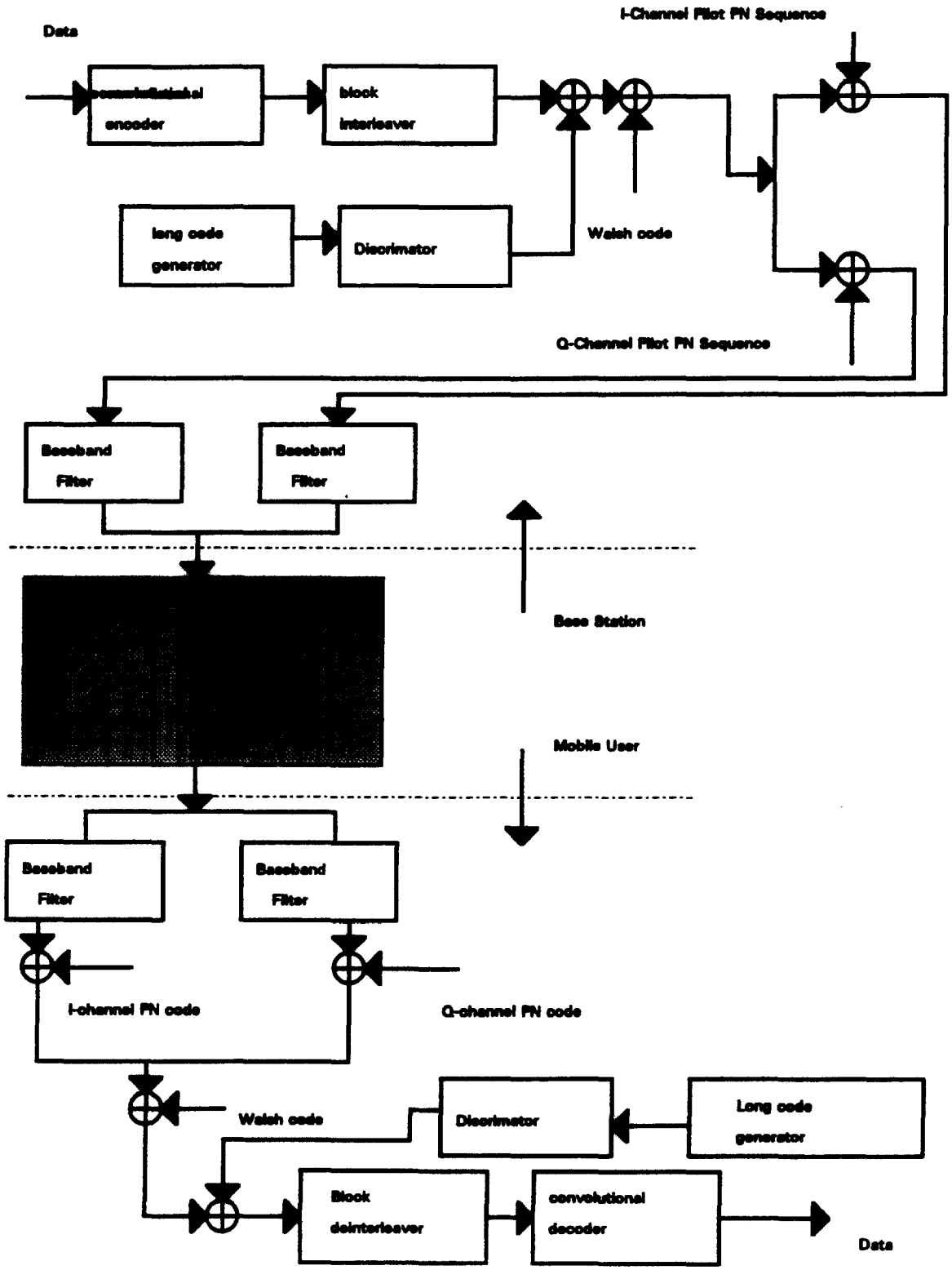

Figure 4.8 Block diagram of the simulated CDMA systems.

4.9 Simulation results

In this section, we present the results of our simulations. The system described in Section 4.8 was simulated using the two-ray channel model discussed in Sections 4.6. and 4.7. for urban and suburban environments. The effects of Doppler shift on BER and FER (Frame Error Rate) are evaluated at several different vehicle speeds. The results of BER and FER for both urban and suburban areas are shown in Figure 4.9 and 4.10 respectively.

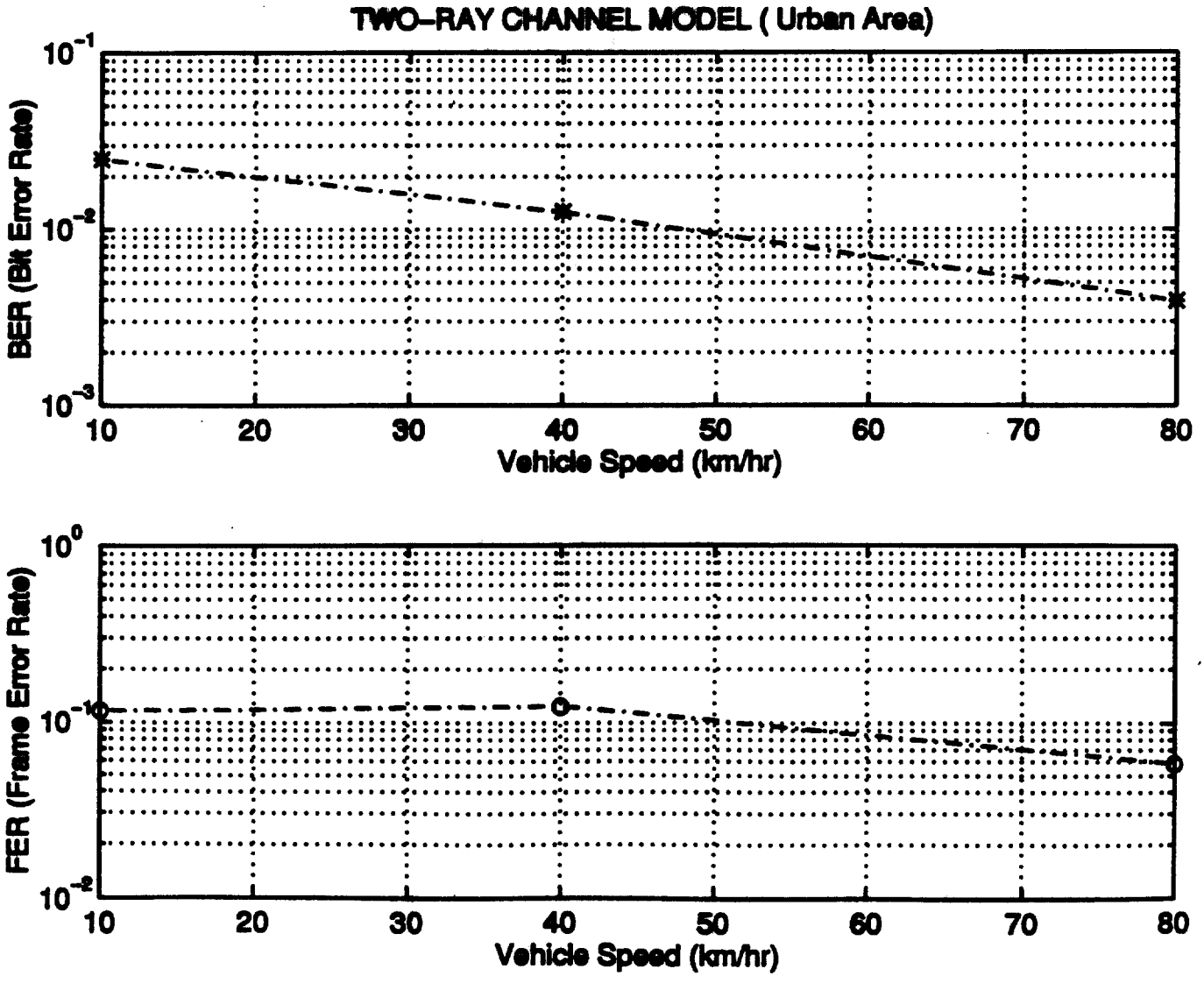

Figure 4.9 BER and FER versus vehicle speed for Eb/No = 10 dB and 20 users.

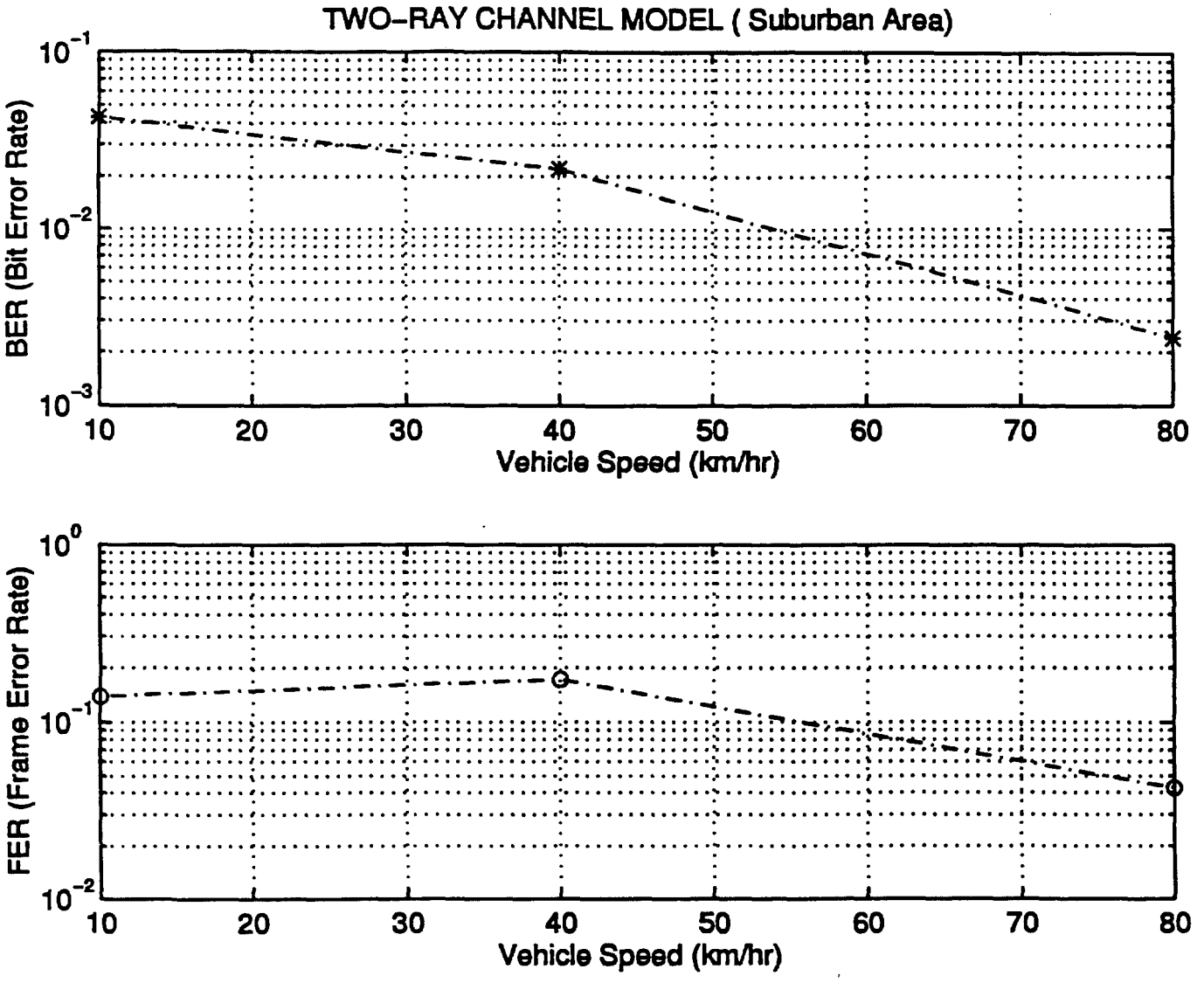

Figure 4.10 BER and FER versus vehicle speed for Eb/No = 10 dB and 20 users.

4.10 Conclusion

Statistical two-ray channel impulse responses with time delays of $\tau = 5 \sim 7$ μs and $\tau = 11 \sim 16$ μs for urban and suburban areas respectively were used in the simulation. The results shown Figure 4.9 and Figure 4.10 suggest that BER and FER decrease as vehicle speed increases. The reason for this is because the interleaver used in the simulated model can successfully break up burst errors caused by Doppler shift and multipath so that errors tend to occur independently. This makes channel increases the effectiveness of the channel coding. For the model employed, the computed BER and FER for the suburban area are slightly greater than those for the urban area.

In order resolve all multipath components, system bandwidth must exceed the coherence bandwidth of the channel [Lee89,Dix84]. Resolution of all significant multipath components requires a system bandwidth of 10 MHz. Beyond 10 MHz, there is no significant improvement. In the range of 1 MHz to 10 MHz, wider bandwidth will result in some modest improvements in multipath rejection [Sch93]. The simulation results presented here indicate that with proper system design, even relatively narrowband spread-spectrum systems can exhibit robust performance over a wide range of channel conditions.

References

[Cla68] R.H. Clarke, "A Statistical Theory of Mobile Radio Reception," *The Bell System Tech. Journal*, pp.957-1000, July-August, 1968.

[Cox73] D. C. Cox, "910 MHz Urban Mobile Radio Propagation: Multipath Characteristics in New York City," *IEEE Trans. Comm.*, Vol. COM-21, no.11, pp.1188-1193, Nov. 1973.

[Dix84] Robert C. Dixon, Spread Spectrum Systems, New York: J. Wiley, 1984.

[Fun91] V. Fung, "Simulation of Bit Error Performance of FSK, BPSK, and $\pi/4$ DQPSK in Flat and Frequency-selective Fading Mobile Radio Channels Using Two-Ray and Measurement-Based Impulse Response Models", *Master Thesis in Electrical Engineering*, Virginia Tech., Blacksburg, VA, 1991.

[Lee89] W. C. Y. Lee, Mobile Cellular Telecommunications, New York: McGraw-Hill, 1989.

[Oss64] J. F. Ossana Jr., "A model for mobile radio fading due to building reflection: theoretical and experimental fading waveform power spectral," *The Bell System Tech. Journal*, pp.2935-2971 Nov. 1964.

[Par89] J. D. Parsons, and J. G. Gardiner, Mobile Communication Systems, Halsted Press, 1989.

[Rap90] T. S. Rappaport, S. Y. Seidel, and R. Singh, "900-MHz Multipath Propagation Measurements for U.S. Digital Cellular Radiotelephone," *IEEE Veh. Tec. Conf.*, pp.131-139, 1990.

[Sch93] D. L. Schilling, "Broadband Spread Spectrum Multiple Access for Personal and Cellular Communications," *1993 IEEE Vehicular Technology Conference*, Secaucus, NJ, pp. 819-826, May 20, 1993.

[Smi75] J. L. Smith, "A computer Generated Multipath Fading Simulation for Mobile Radio," *IEEE Trans. Veh. Tech.*, VT-24, no.3, pp.39-40, August 1975.

5 Limitations of Practical RF Systems

5.1 Analysis of nonlinearities within receiver

An amplifier may have non-linear characteristics, which are a significant source of errors in some communications systems. When the input signal is small, only a small part of the transconductance curve is used and amplification takes place over an almost linear arc of the curve. However, when the signal is large and varies over a broad range, the operation is no longer linear. Such a non-linearity results in the distortion of the output waveform, called harmonic distortion. The output waveform can be expressed as

$$y(t)=M_0+M_1\cos(\omega t)+M_2\cos(2\omega t)+M_3\cos(3\omega t)+\cdots, \tag{5.1}$$

where M_1 is the amplitude of the fundamental component of the output wave, and M_2, M_3, M_4 are the amplitudes of the second, third, and fourth harmonic, respectively.

In the proposals filed with the FCC, some companies advocate the allocation of two sub-bands within the ISM band, at 904-912 MHz and 918-926 MHz. Since the corresponding CDMA carrier frequencies are 908 MHz and 922 MHz, the input signal can be represented as

$$y_1(t)=I_1(t)\cos\omega_1 t+I_2(t)\cos\omega_2 t. \tag{5.2}$$

After amplification, the output signal can be represented by its harmonic components:

$$y_1(t)=M_1I_1(t)\cos\omega_1 t+M_2I_2(t)\cos\omega_2 t. \tag{5.3}$$

$$y_2(t)=M_2\left[\frac{I_1^2}{2}+\frac{I_2^2}{2}+\frac{I_1^2}{2}\cos 2\omega_1 t+\frac{I_2^2}{2}\cos 2\omega_2 t+I_1I_2\cos(\omega_1+\omega_2)t+I_1I_2\cos(\omega_1-\omega_2)t\right] \tag{5.4}$$

$$y_3(t)=\frac{M_3I_1^3}{4}(3\cos\omega_1 t+\cos 3\omega_1 t)+\frac{3M_3I_1^2I_2}{2}\left[\cos\omega_2 t+\frac{1}{2}\cos(2\omega_1+\omega_2)t+\frac{1}{2}\cos(2\omega_1-\omega_2)t\right]$$

$$+\frac{3M_3I_2^2I_1}{2}\left[\cos\omega_1 t+\frac{1}{2}\cos(2\omega_2+\omega_1)t+\frac{1}{2}\cos(2\omega_2-\omega_1)t\right]+\frac{M_3I_2^3}{4}(3\cos\omega_2 t+\cos 3\omega_2 t) \tag{5.5}$$

In the above expressions, $y_1(t)$ is just the amplified input signal, while $y_2(t)$ and $y_3(t)$ are the harmonic and intermodulation products. Harmonic components of frequency f_1 and f_2 occur at $2f_1$, $2f_2$, $3f_1$, $3f_2$ etc. The first harmonic terms are $\frac{I_1^2}{2}\cos 2\omega_1 t+\frac{I_2^2}{2}\cos 2\omega_2 t$.

In the output signal, sums and differences of harmonics of f_1 and f_2 can be $f_1 - f_2$, $f_1 + f_2$, $2f_1 - f_2$, $2f_2 - f_1$, etc. These terms are called intermodulation distortion. The output terms $I_1 I_2 \cos(\omega_1 + \omega_2)t + I_1 I_2 \cos(\omega_1 - \omega_2)t$ are called the second order intermodulation products and the output terms with the form $\frac{3M_2 I_1^2 I_2}{2}[\frac{1}{2}\cos(2\omega_1 + \omega_2)t + \frac{1}{2}\cos(2\omega_1 - \omega_2)t]$ are called the third order intermodulation products. Spectral analysis of the output signal indicates that:

- The desired fundamental signal output power is $\propto I_n$,
- The second order intermodulation output is $\propto I_n^2$,
- The third order intermodulation output is $\propto I_n^3$.

For $f_1 = 908 MHz$, $f_2 = 922 MHz$ there are no harmonic components falling into the 902-926 MHz ISM band.

Some other proposals also suggest FCC to allocate the ISM band into four bands, which are 904 - 908 MHz (Band A), 908 - 912 MHz (Band B), 918 - 922 MHz (Band C), and 922 - 926 MHz (Band D). The carrier frequencies of those bands will be 906, 910, 920, 924 MHz, respectively. For these carrier frequencies, it is impossible for any second or fourth order intermodulation components to appear in 902 - 928 MHz ISM band. It is possible that some third order intermodulation components may exist in the ISM band. They are $2f_2 - f_1 = 914\ MHz$ and $2f_4 - f_3 = 916 MHz$. However, third order intermodulation components will only cause interference in 912 - 916 MHz and 914 - 918 MHz frequency bands. Fortunately, these intermodulation products fall outside the four proposed frequency bands.

According to the above analysis, for both allocation proposals, there will not be any second or third intermodulation distortion present in the operating frequency bands. In other words, non-linear amplification should not pose significant problems with the proposed AVM frequency allocations.

5.2. Spectrum sharing

CDMA is a modulation and multiple access scheme based on spread spectrum techniques. Unlike frequency division multiple access (FDMA) in which signals are assigned narrow band frequency slots, and time division multiple access (TDMA) in which signals are assigned specific time slots, CDMA signals are modulated with a pseudo-random binary sequence which spreads the signal energy over the a wideband. This technique allows a large number of CDMA signals to share the same spectrum, as discussed in Section 3. The signals are separated at the receiver using a correlator which multiplies the incoming signal by a time-synchronized replica of the spreading code. This removes the spreading codes from the received signal and rejects other CDMA signals.

The capacity and overall quality of a CDMA system are maximized through the use of power control. Link quality is maintained and interference to other users is minimized by controlling the transmit power of each mobile station such that each signal arrives at the cell site with the minimum required signal-to-noise ratio. To achieve this, two types of power control can be used: open loop and closed loop. Open loop power control is primarily used by the mobile station (MS). The purpose of open loop power control is to provide rapid transmit power adjustment according to changes in received power from the base station. The MS transmit power is adjusted directly using estimates of the received signal strength.

Closed-loop power control is performed by the base station (BS). The BS measures the received E_b/N_0 from each mobile and commands the mobile transmitter to adjust its power according to a threshold, which is dependent upon the frame error rate (FER) of the link. The purpose of closed-loop power control is to provide corrections to the open loop estimates in order to maintain the optimal transmit power for a desired FER.

The design of spread-spectrum networks requires methods that differ dramatically from the design of narrowband networks. One of the key factors is that the geographical distribution of users has an influence on the coverage and capacity of CDMA. No matter which AVM system is used, power control for each user is important for maximizing system capacity.

If there is more than one system using the same frequency band, it would be extremely difficult to have adequate power control among users from disparate systems. Without good power control, the overall system capacity suffers from severe degradation. Also, different systems would need to coordinate the spreading sequences which are assigned to each user. Therefore, sharing the same frequency band does not appear to be practical.

An alternative is to place AVM systems in adjacent bands. It is possible to locate the main lobe of one system's spectrum over a sidelobe of a second system's spectrum. This would allow efficient spectrum usage and mitigate the interference between systems. To realize a partial overlay system, spectral shaping techniques would be employed to minimize the sidelobe effects on the adjacent channels.

5.3. Sidelobe effect estimation

A general RF path loss model for the mobile to base station link is shown below:

$$L_p = 147.5 - 20\log h_1 h_2 + 40\log d: \qquad (5.6)$$

where h_1, h_2 represent the heights of the transmit and receive antennas, d is the distance in miles, and L_P is the path loss is dB.

In an urban environment, the coverage radius of a cell site might be around 1-3 miles. Consider the case in which a mobile unit operates from the edge of the coverage region and at the same time another mobile unit from adjacent system is operating close to the base station antenna. Obviously, the base station will receive a higher power level from the nearby signal than from the distant signal. For instance, if one user is transmitting from 3 miles away and a user from another system is transmitting from 0.3 miles away and with equal signal power, the non-system user's signal will dominate the received signal According to the RF propagation loss model, the signal strength difference at base station antenna could be as much as 40 dB.

In a rural area, a cell site usually has 5-8 miles line of sight coverage. In a worst case scenario, a nearby mobile unit might be 0.5 miles away from base stations, and a distant mobile unit might be 7.5 miles away. Thus, the signal strength difference could be as high as 47 dB.

5.4. Spectral shaping filtering

As proposed by some companies, the ISM band could be allocated into four 4 MHz sub-bands. However, this may result in the sidelobes of one system leaking into adjacent channels and causing adjacent channel interference. The unfiltered power spectral densities of BPSK and QPSK consist of a main lobe and a series of side lobes.

In order to reduce the effects of the sidelobes, the modulated signal should be filtered to minimize the sidelobe before transmission. Some filtering techniques can reduce energy in the sidelobes of BPSK and QPSK dramatically, to as low as -35 dB. However, in order to avoid significant distortion of the mainlobe or costly filters, filtering should reduce sidelobe energy to -25 dB. Figures 5.1 and 5.2 compare the power spectrum between the original CDMA signal and the filtered CDMA signal. A DS-SS signal with a 4 MHz bandwidth is represented in complex baseband form. Figure 5.1 shows the power spectrum of original CDMA signal, while Figure 5.2 shows the power spectrum of CDMA signal after filtering. The peak of sidelobe of the filtered signal is approximately -24 dB down from the peak of mainlobe signal.

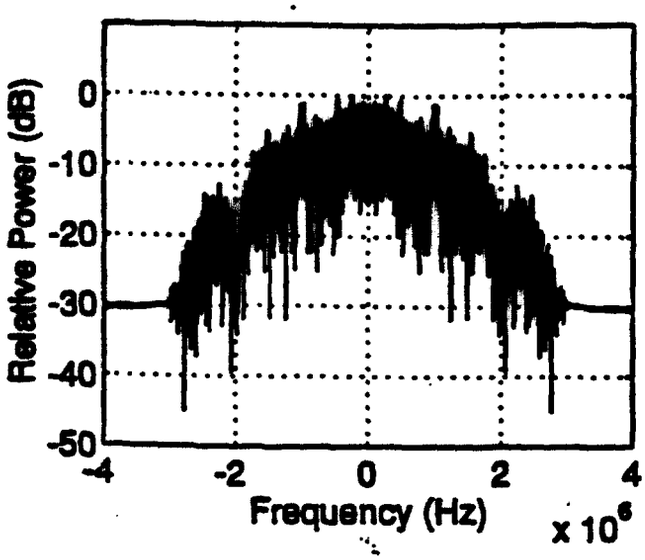

Figure 5.1
Power spectrum of unfiltered CDMA signal

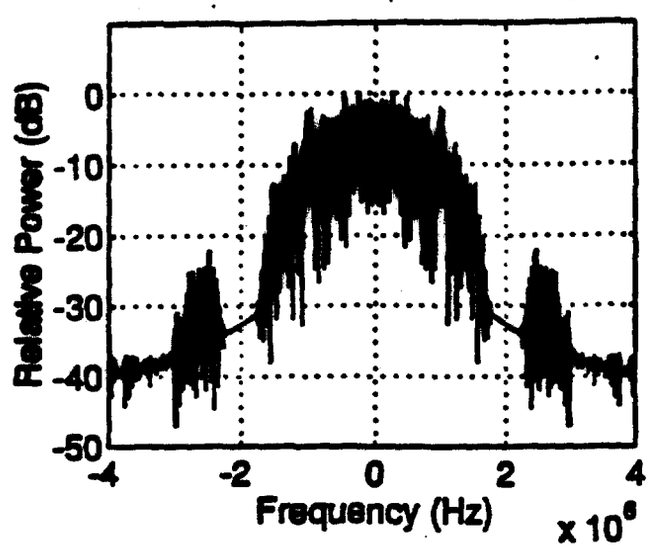

Figure 5.2
Power spectrum after spectrum shaping filtering

Although spectral shaping filters can greatly reduce the sidelobe energy, they may also introduce distortion. Generally, a higher order filter is used for minimizing the distortion. However, in this case the distortion caused by spectral shaping filtering is limited to a small portion of spectrum that are close to edge of band. Some interference rejection techniques, such as the Time-Dependent-Adaptive-Filter (TDAF), have a significant interference mitigation capability. The theoretical background and performance of the TDAF is shown in the next chapter. Simulation results shows that a CDMA signal distorted by spectral shaping filtering can be improved by using TDAF processing. Therefore, a high order or expensive filter is not necessary to perform the spectral shaping.

5.5 Summary

According to our analysis, nonlinearities within amplifiers should have little impact on ISM band AVM system signals if frequency bands are allocated properly For ISM band spread-spectrum AVM systems, direct overlay of different AVM systems in the same frequency band relies on power control among all users. However, coordinated power control between different systems does not seem practical. On the other hand, it may be feasible to locate the mainlobe of one AVM system over a sidelobe of a second system. For partial overlay systems, spectral shaping filtering is required before transmission to reduce adjacent channel interference. Although spectral shaping could introduce distortion into a spread-spectrum signal, the signal can be recovered by using advanced DSP techniques, such as TDAF processing, considered in the next section.

6 Interference Rejection Techniques for AVM Systems

Spread-spectrum systems present a challenging environment for interference mitigation. In addition to the traditional sources of interference such as noise and multipath, CDMA systems suffer from interference attributed to other users of the same frequency band. This multiple access interference severely limits the capacity and spectral efficiency of CDMA systems, as discussed in previous sections Additionally, AVM systems in the ISM band must combat interference from dissimilar modulation formats. If interference rejection is primarily obtained by the processing gain of the spread-spectrum modulation, then the system capacity is constrained by the available processing gain. The current generation of CDMA systems employs single stage correlation receivers that correlate the received signal with a synchronized copy of the desired signal's spreading code. Greater channel capacity for CDMA can be achieved by using interference rejection techniques.

6.1.1 Interference rejection techniques for direct sequence spread spectrum systems

If after spreading the spectrum of the underlying information over the maximum bandwidth available to the system, the resulting interference rejection capability is still not large enough to sufficiently attenuate any undesired signal, additional techniques for interference removal must be employed. Notch filters are one popular technique for narrow-band interference rejection. Two techniques have received the most interest. The first technique is to use a tapped delay to implement either a one-sided prediction-error filter (Weiner filter) as described in [Ilt78], or a two-sided filter. The rationale for the use of the Weiner prediction filter for narrow-band interference suppression is the following. The incoming waveform to the spread spectrum receiver consists of the desired spread spectrum signal, thermal noise, and the narrow-band interference. Since both the DS/SS signal and the thermal noise are wide-band processes, their future values cannot be readily predicted from their past values. On the other hand, future values of the narrow-band interference process, can indeed be predicted from past values. Hence, the current value, once predicted, can be subtracted from the incoming signal, leaving a waveform comprised primarily of the DS/SS signal, and the thermal noise. The same general philosophy holds for the two-sided transversal filter, except now the estimate of the present value of the interference is based upon both past and future values, and the improvement in system performance alluded to above is due to the use of both to estimate the present.

Another narrow-band interference rejection technique is transform domain processing (TDP), as described in [Mil88]. This technique uses a tapped delay line to take the Fourier Transform in real time. The tapped delay line is typically implemented with a surface acoustic wave (SAW) device with. A notch filter is implemented by Fourier transforming the received waveform, using an on-off switch to perform the notching operation, and then inverse transforming the signal.

Both techniques can use tapped delay-line implementations, and both can be made adaptive. In the former scheme, the system can be made adaptive by using a tapped delay line with variable tap weights. These tap weights can be adapted, for example, by using the well-known least-mean-square (LMS) algorithm. In the latter technique, an envelope detector in cascade with a threshold-crossing indicator can be used to determine the location of the narrow-band interference, and adjust the position of the notch (or notches) to suppress the interference.

One general problem associated with the actual implementation of either of these two systems is that of dynamic range. Since these systems are intended to operate in large interference environments, the range of input levels that SAW devices can handle is crucial.

It appears that each of these schemes has its own set of advantages and disadvantages for specific scenarios. For example, consider the simple example of a sine wave interferer at a known frequency. Whereas the estimation-type filter can, if desired, put a zero at the frequency of the sine wave and hence null it out completely, this complete nulling is typically not possible for the TDP receiver. Because the input to the TDP receiver is windowed in time before it is Fourier transformed, sidelobes are immediately put on the interference spectrum, and even an infinitely deep notch over some appropriate fraction of the bandwidth of the system will not completely eliminate the interference. However, the TDP system can be made adaptive on a nearly "instantaneous" basis, without the need for an adaptive algorithm with its attendant convergence problems. As a result, the TDP receiver has an advantage over the receiver employing an estimation filter in those cases where rapid adaptivity is required.

6.1.2 Interference rejection techniques for CDMA

There are two categories of CDMA interference rejection techniques. The first category encompasses algorithms which exploit the cyclostationary properties of spread-spectrum signals. In many instances, these algorithms resemble fractionally-spaced equalizers (FSE). The second class of techniques uses multiple stage correlation receivers to estimate and subtract the multiple access interference.

Monogiousids, Tafazolli, and Evans [Mon93] employ a technique based on adaptive linear fractional spaced equalization (LFSE) to adaptively cancel the multiple access interference in CDMA systems. The simulation results indicate that the LFSE offers significant gains over the conventional detector, eliminating the near-far problem without explicit knowledge of the interfering spreading sequences.

Rapajic and Vucetic [Rap93] describe a fully asynchronous single user receiver for a CDMA system where the receiver is trained by a known training sequence prior to data transmission, and is continuously adjusted by an adaptive algorithm during data transmission. An adaptive, fractionally-spaced LMS filter, instead of matched filters with

constant coefficients is employed at each user's receiver. Experimental results show that a considerable improvement in BER is achieved with respect to the conventional single-user receiver. Abjurahuman, Falconer, and Sheikh [Abj92] present related work on fractionally-spaced DF minimum mean squared error (MMSE) filters for DS/SS CDMA. They have demonstrated that an FSE can be used as a CDMA demodulator even when slow fading is present. The advantage of this receiver is its simplicity.

Madhow and Honig [Mad93] consider interference suppression schemes for DS/SS CDMA systems using the MMSE criterion. These schemes have the virtue of being amenable to adaptation and are simple to implement, while alleviating the near-far problem to a large extent. The channel output is first passed through a filter matched to the chip waveform and then sampled at the chip rate. Because of the complexity and coefficient noise associated with such an adaptive when N is large, simper structures with fewer adaptive components have been proposed. In each case, multiple samples per symbol are combined via a tapped delay line, where the taps are selected to minimize the mean square error.

Holley and Reed [Hol92] and also Aue and Reed [Aue94] show how spectral correlation properties can be exploited by a time-dependent adaptive filter (TDAF) to provide spectral capacity for CDMA using frequency-domain and time-domain filtering structures. Their research suggests that by using TDAF processing, CDMA systems can approach the same spectral efficiency as FDM/TDM systems while maintaining the advantages of wide-band modulation and universal frequency reuse.

Asynchronous CDMA systems using digital matched filtering (DMF) reception techniques suffer from poor multiple access spectral efficiency. This is due primarily to the lower bounds on the mean square cross-correlation levels which exist between the spreading codes allocated to each system subscriber. This interference can be estimated through channel measurement, and it is then possible to regenerate and subsequently cancel cross-correlation components from individual interfering channels.

Multi-stage correlation receivers, due to Varansi and Azhang [Var90], are a promising suboptimal approach for reducing interference and increasing channel capacity. At each stage, a bank of single-user receivers demodulates the received signal. After each stage, the estimated signals for all interference sources are subtracted from the received signal, and then demodulation is repeated. This procedure can be repeated for an arbitrary number of stages to obtain an iterative estimate of the interference. Simulation results for a simple channel model indicate that only a few stages are necessary to achieve most of the potential performance improvement.

Most work on multistage interference rejection techniques has focused on idealized Gaussian channels and assumes perfect knowledge of each user's power. In order for multi-stage receivers to perform well on the time-varying multipath channels, it is necessary to estimate the channel characteristics. The use of a RAKE receiver (or similar adaptive channel estimator) in a multi-stage algorithm makes this possible. The RAKE

can be used to simultaneously estimate the received data and the channel impulse response for each user with no prior information about the channel conditions. An estimate of the received signal from each user can then be constructed and subtracted from the actual received signal [Str94].

6.2 Time-dependent adaptive filter

The Time Dependent Adaptive Filter (TDAF) represents one particularly promising alternative to matched filter processing of CDMA signals. For example, time dependent filtering is able to mitigate many different forms of interference common to the mobile channel. Furthermore, time-dependent filtering requires no prior knowledge of the other users in the system in order to produce marked increases in user capacity.

6.2.1 Theoretical background of time dependent adaptive filter

In order to realize any benefit from time dependent filtering, either the desired signal or the interfering signals must exhibit the property of cyclostationarity. Cyclostationarity is a term which is used to describe the repetitive or cyclic nature of the statistics associated with a communications signal.

A process $x(t)$ is said to be cyclostationary in the wide sense if its mean and autocorrelation $R_x(t,u)$ are periodic with some period, say T_0. The time-dependent autocorrelation of $x(t)$ is

$$R_x(t-\tau/2, t+\tau/2) = \sum_{-\infty}^{\infty} R_x^{\frac{n}{T_0}}(\tau) e^{j2\pi\frac{n}{T_0}t}. \tag{6.1}$$

The variable t represents time, τ represents the lag, and T_0 represents the period of the cyclostationarity and $1/T_0$ is the cycle frequency. For most digital modulation schemes, T_0 represents the period of a baud or half the period of the carrier. Often, it is useful to define the set of cycle harmonics which are integrally related to the fundamental periodicity, T_0, as $\alpha = \frac{n}{T_0}$, where n is an integer number. Using this notation, the coefficients for the harmonic components of the cyclic autocorrelation function are given by

$$R_{xx}^{\alpha}(\tau) = \frac{1}{T_0} \int_{-T_0/2}^{T_0/2} R_{xx}(t,\tau) e^{-j2\pi\alpha t} dt. \tag{6.2}$$

Furthermore, if the range of n represents the complete set of harmonics which are integrally related to the fundamental periodicity, then the total autocorrelation may be expressed in terms of it's Fourier series expansion:

$$R_{xx}(t,\tau)=\sum_{-\infty}^{\infty}R_{xx}^{\alpha}(\tau)e^{j2\pi\alpha t}. \tag{6.3}$$

The Fourier transform of the cyclic autocorrelation is called the cyclic spectrum and is defined as

$$S_{xx}^{\alpha}(f)=\int_{-\infty}^{\infty}R_{xx}^{\alpha}(\tau)e^{-j2\pi f\tau}d\tau. \tag{6.4}$$

Similarly, the time dependent spectral density is given as

$$S_{xx}(t,f)=\int_{-\infty}^{\infty}R_{xx}(t,\tau)e^{-j2\pi f\tau}d\tau. \tag{6.5}$$

These quantities provide a measure of spectral correlation between frequency components in a signal. In particular, the cyclic spectral density, $S_{xx}^{\alpha}(f)$, provides a measure of the correlation between frequency components at $f-\alpha/2$ and $f+\alpha/2$. This fact is most clearly seen by taking the Fourier transform of a finite window of data,

$$X_W(t,f)=\int_{t-\frac{W}{2}}^{t+\frac{W}{2}}x(u)e^{-j2\pi fu}du, \tag{6.6}$$

and using the linearity property of the Fourier transform to rewrite $S_{xx}^{\alpha}(f)$ as

$$S_{xx}^{\alpha}(f)=\lim_{W\to\infty}\lim_{T\to\infty}\frac{1}{T}\int_{-T/2}^{T/2}\frac{1}{W}E\langle o\rangle dt, \tag{6.7}$$

where $E\langle o\rangle=E\left\langle X_W(t,f+\frac{\alpha}{2})X_W^*(t,f-\frac{\alpha}{2})\right\rangle$. In this form, it is clear that the cyclic spectral density provides a clear measure of both the location and degree of spectral correlation in a cyclostationary process.

6.2.2 Spectral correlation in direct-sequence spread spectrum modulation

For a direct sequence spread spectrum system (DS/SS), the input data signal $d(t)$ is spread in bandwidth by multiplication with a high rate chip signal $c(t)$. This can be viewed

as the multiplication of a low-rate cyclostationary process by a high-rate cyclostationary process. There exist three fundamental periodicities in direct sequence spread spectrum signals:

- the fundamental chip rate periodicity, T_{chip} ,
- the fundamental data rate periodicity, T_{data} ,
- the fundamental code repetition rate periodicity, T_{code} .

A high degree of spectral correlation can be achieved in a DS/SS signal by carefully choosing the relationships between the three fundamental periodicities. Traditionally, the period of a data baud is chosen as an integer multiple of the chip period. Although not required, this choice insures minimal spectral "splashing" and maximum in-band power utilization. Similarly, the code repetition rate can be designed to provide a high degree of spectral correlation. In fact, if the code repetition period is designed to be an integer multiple of the chip rate period, then the degree of spectral correlation is greatly enhanced.

When both the data and code repetition rates are designed to be integrally related to the chip rate, the number of fundamental periodicities in the DS/SS signal is reduced to one. Specifically, if S is defined as the number of chips per baud and M is defined as the number of chips per code sequence repetition, then the fundamental cycle frequencies become functions of a single fundamental periodicity, T_{chip}.

$$\alpha_{chip} = \frac{1}{T_{chip}} \tag{6.8}$$

$$\alpha_{data} = \frac{1}{T_{data}} = \frac{1}{ST_{chip}} \tag{6.9}$$

$$\alpha_{code} = \frac{1}{T_{code}} = \frac{1}{MT_{chip}} \tag{6.10}$$

The parameter S is known as the spreading or processing gain of the DS/SS signal. In order to best exploit the spectral correlation of DS/SS, the data rate and code repetition rate should be integrally related, - i.e., either the ratio $\frac{S}{M}$ or the ratio $\frac{M}{S}$ must be an integer.

6.2.3 Time dependent adaptive filter (TDAF) for CDMA interference rejection

The basic approach of TDAF structures is to convert a single cyclostationary process into a collection of spectrally correlated processes. Optimal filtering is then accomplished through the optimal combination of the spectrally correlated processes to estimate each and every spectral correlation process.

The idea behind the TDAF is to minimize the time-averaged difference between a desired frequency component and a linear combination of correlated frequency

components. By filtering correlated frequency components of the corrupted input signal and combining these components appropriately, a better estimate of the uncorrupted signal can be obtained.

Mathematically, this is seen by taking a finite window Fourier transform of the received data

$$X_T(t,f) = \int_{t-T/2}^{t+T/2} x(\tau)e^{-j2\pi f\tau}d\tau, \tag{6.11}$$

where T is the window length. Assuming that an uncorrupted version of the transmitted signal, $Y_T(t,f)$, is available (i.e., - a training or desired signal), the error after filtering can be computed as

$$\varepsilon_T(t,f) = Y_t(t,f) - \sum_{n=0}^{M-1} W_n(f)X_T(t,f-\alpha_n). \tag{6.12}$$

The objective is to determine the filters $W_n(f)$ which minimize the mean square error (MSE):

$$\text{minimize} \quad MSE = \lim_{T\to\infty} \frac{1}{T}\int_{-T/2}^{T/2} [\varepsilon_T(t,f)]^2 dt. \tag{6.13}$$

In this equation, α_n represents the range of fundamental cycle frequencies available to the filter. The optimal filter is designed by setting the derivative with respect to $W_n(f)$ equal to 0:

$$0 = \lim_{T\to\infty} \frac{1}{T}\int_{-T/2}^{T/2} [\varepsilon_T(t,f)]X_T^*(t,f-\beta)dt. \tag{6.14}$$

When T is allowed to become large, the solution becomes:

$$\sum_{n=0}^{M-1} W_n(f)\hat{S}_{xx}^{\alpha-\alpha_n}(f-\frac{\alpha_n+\beta}{2}) = \hat{S}_{yx}^{\alpha}(f-\frac{\beta}{2}), \tag{6.15}$$

where $\hat{S}_{xx}^{\alpha-\alpha_n}(f)$ and $\hat{S}_{yx}^{\alpha}(f-\frac{\beta}{2})$ represent finite time approximations of their respective cyclic spectral densities. The design of the TDAF consists of a bank of filters $W_n(f)$, each of which filters a frequency-shifted version of the input signal. The output of the TDAF is a sum of frequency-shifted and filtered signals.

An ideal frequency response may require a large number of frequency shift processing and filters. Too many phase lock oscillators and FIR filters could be very inefficient in

computation. In order to minimize the overall computational count, the Discrete Fourier Transform (DFT) can be used in place of the phase locked complex oscillators and filters to achieve the necessary frequency translation and filtering of the spectrally correlated components. If the sampling rate is chosen to be a multiple of the chip rate, then an appropriate DFT size can be chosen to exploit the spectral correlation. The preferred structure for the optimal time dependent filter of a DS-SS signals is shown in Figure 6.1.

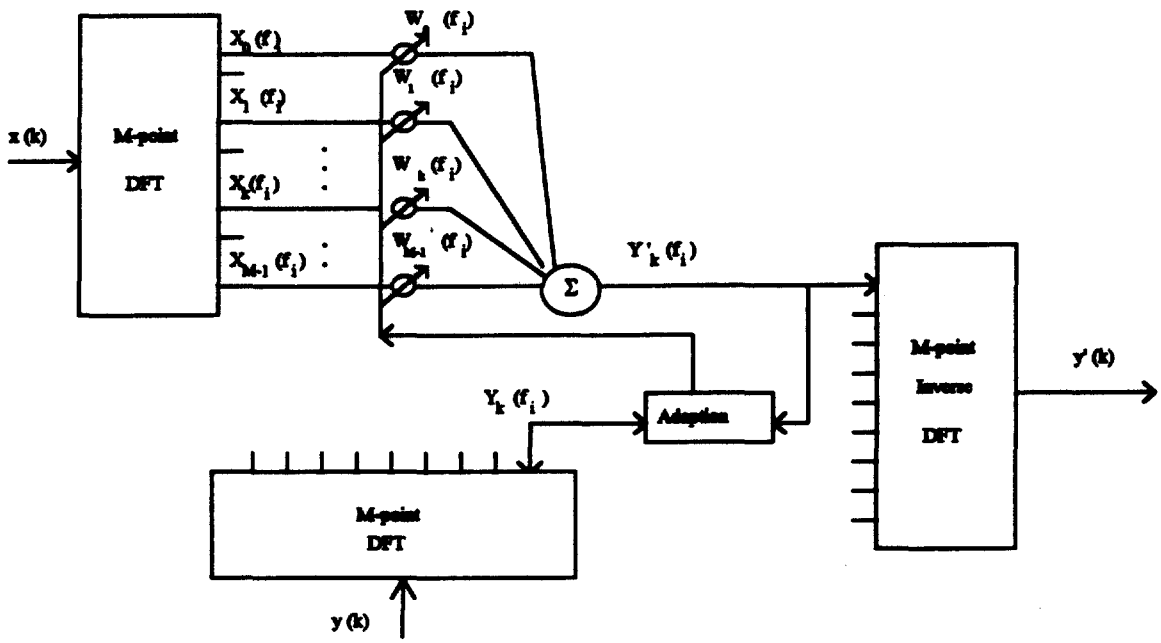

Figure 6.1 FFT based optimal Time Dependent Adaptive Filter structure showing the estimation of one output bin

6.2.4 RLS adaptation of the TDAF

Least Mean Squares (LMS) adaptation algorithm usually requires minimal computation and hardware, however it is often slow to converge, especially when the number of weights is large. Normalized and accelerated LMS algorithms attempt to decrease the LMS convergence time by adapting the step size. But the improved convergence rate is still too slow to track a dynamic mobile channel when applied to TDAF structures.

Compared to the LMS algorithm, the Recursive Least Squares (RLS) algorithm is very attractive due to its fast convergence, relative insensitivity to the eigenvalue spread,

and lower steady-state mean square error. The major drawbacks of the RLS algorithm are its increased computation count and storage requirements. The RLS algorithm can be utilized for time-dependent filtering to adaptively combine spectrally correlated portions of the signal spectrum in the following manner.

The RLS adaptation algorithm attempts to minimize the least squares error between a desired frequency component and a linear combination of correlated frequency components. It is assumed that the sample rate of the input signal is an integer multiple of the fundamental code repeat rate. The transformed input vector is then given by

$$X_k(f_i) = i\text{'th bin FFT } [x(k)\ x(k-1)\ \cdots\ x(k-N+1)]^T. \tag{6.16}$$

The corresponding weight vectors will be a row of a single $N \times N$ matrix:

$$W_k^0 = \begin{vmatrix} W_{0,0}^0 & W_{0,1}^0 & \cdots & W_{0,N-1}^0 \\ W_{1,0}^0 & W_{1,1}^0 & \cdots & W_{1,N-1}^0 \\ \cdot & & & \cdot \\ \cdot & & & \cdot \\ W_{N-1,0}^0 & W_{N-1,1}^0 & \cdots & W_{N-1,N-1}^0 \end{vmatrix}. \tag{6.17}$$

The inverse spectral correlation matrix R_{k-1}^{-1} of the TDAF are initialized as

$$R_{k-1}^{-1} = \eta \cdot I, \tag{6.18}$$

where η is chosen as a large positive constant and I represents the $N \times N$ identity matrix. The elements of the a priori frequency-domain output bins are computed in scalar form as

$$\hat{Y}_k^a(f_i) = \sum_{n=-l}^{u} W_{k-1,n}^0(f_i) \cdot X_{k,n}(f_i + \alpha_n). \tag{6.19}$$

The range of n is defined to be $n \in \{-l, u\}$ so that $X_k(f_i + \alpha_{-l})$ and $X_k(f_i + \alpha_u)$ lie within the possible FFT bins. In matrix form, it can represented as the product of the weight matrix and the input FFT bins

$$\hat{Y}_k^a = W_{k-1}^0 X_k. \tag{6.20}$$

In this form, each bin of $\hat{Y}_k^a$ is formed from a linear combination of all the input bins. After forming the priori output estimate, the frequency-domain error vector is computed as

$$E_k = Y_k - \hat{Y}_k^a, \tag{6.21}$$

or in scalar form as

$$E_k(f_i) = Y_k(f_i) - \hat{Y}_k^a(f_i). \tag{6.22}$$

The frequency-domain gain vector is then computed based on the vector product of the inverse spectral correlation matrix and the current frequency-domain input vector. The complete RLS adaptation algorithm for TDAF is presented in Table 6.1.

Table 6.1 RLS adaptation algorithm for TDAF

$$W_{k-1}^0 = 0 \cdot I$$
$$R_{k-1}^{-1} = \eta \cdot I$$
$$X_k(f_i) = i\text{'th bin of } FFT\,[x(k)\ x(k-1) \cdots x(k-N+1)]^T$$
$$\hat{Y}_k = W_{k-1}^0 X_k$$
$$E_k = Y_k - \hat{Y}_k$$
$$Z_k = X_k^H R_{k-1}^{-1}$$
$$Q = Z_k X_k$$
$$V = \frac{1}{\rho + Q}$$
$$\tilde{Z}_k = V \cdot R_{k-1}^{-1} X_k$$
$$R_k^{-1} = \frac{1}{\rho}[R_{k-1}^{-1} - \tilde{Z}_k Z_k]$$
$$W_k^0 = W_{k-1}^0 + E_k \tilde{Z}_k^H$$
$$[\tilde{y}^a(k)\ \tilde{y}^a(k-1) \cdots \tilde{y}^a(k-N+1)]^T = FFT^{-1}[\hat{Y}_k]$$
$$[\tilde{y}^p(k)\ \tilde{y}^p(k-1) \cdots \tilde{y}^p(k-N+1)]^T = FFT^{-1}[W_k^0 X_k]$$

After convergence of the TDAF, the output approximates the desired signal. At this stage, a maximum likelihood estimate of the desired signal can be obtained from the output signal. This estimate constitutes a non-training sequence directed adaptation criterion for adaptively tracking changes in the input process.

The algorithm for blind adaptation of a time dependent filter is very similar to the adaptation algorithm when training sequences are used. The modification required is to replace the ideal input $y(k)$ with the estimate of correct symbol S_c. The best estimate of correct symbol is obtained by making a maximum likelihood estimate based on the filter output. For binary systems, the valid symbol would be either +1 or -1. By using a best estimate S_c as the training or desired sequence $y(k)$, the RLS adaptation algorithm in Table 6.1 is easily to be modified to form a blind adaptation algorithm.